1

Kirrel3-mediated synapse formation is attenuated by disease-associated missense variants

Abbreviated Title: Kirrel3 variants impair its function

Matthew R. Taylor[1*], E. Anne Martin[1*], Brooke Sinnen[1], Rajdeep Trilokekar[1], Emmanuelle Ranza[2,3], Stylianos E. Antonarakis[2,4], Megan E. Williams[1]

[1]Department of Neurobiology and Anatomy, University of Utah School of Medicine, Salt Lake City, UT 84112, USA
[2]Service of Genetic Medicine, Geneva University Hospitals, Geneva, Switzerland
[3]Current address: Medigenome, Swiss Institute of Genomic Medicine, Geneva, Switzerland
[4]Department of Genetic Medicine and Development, University of Geneva Medical Faculty, Geneva, Switzerland
* These authors contributed equally to this work

Correspondence should be addressed to Megan E. Williams at megan.williams@neuro.utah.edu.

Number of pages: 37
Number of figures: 6
Number of tables: 1
Abstract word count: 209
Introduction word count: 728
Discussion word count: 1562

Conflict of Interest Statement: The authors declare no competing financial interests.

35 **ABSTRACT**

36   Missense variants in Kirrel3 are repeatedly identified as risk factors for autism spectrum

37 disorder and intellectual disability but it has not been reported if or how these variants disrupt Kirrel3

38 function. Previously, we studied Kirrel3 loss-of-function using knockout mice and showed that Kirrel3 is

39 a synaptic adhesion molecule necessary to form one specific type of hippocampal synapse in vivo. Here,

40 we developed a new gain-of-function assay for Kirrel3 and find that wild-type Kirrel3 induces synapse

41 formation selectively between Kirrel3-expressing cells via homophilic, trans-cellular binding. We tested

42 six disease-associated Kirrel3 missense variants and find that five attenuate this synaptogenic function.

43 All variants tested traffic to the cell surface and localize to synapses similar to wild-type Kirrel3. Two

44 tested variants lack homophilic trans-cellular binding, which likely accounts for their reduced

45 synaptogenic function. Interestingly, we also identified variants that bind in trans but cannot induce

46 synapses, indicating Kirrel3 trans-cellular binding is necessary but not sufficient for its synaptogenic

47 function. Collectively, these results suggest Kirrel3 functions as a synaptogenic, cell-recognition

48 molecule, and this function is attenuated by missense variants associated with autism spectrum disorder

49 and intellectual disability. Thus, we provide critical insight to Kirrel3 function in typical brain

50 development and the consequences of missense variants associated with autism spectrum disorder and

51 intellectual disability.

52

53 **SIGNIFICANCE STATEMENT**

54   Here, we advance our understanding of mechanisms mediating target-specific synapse

55 formation by providing evidence that Kirrel3 trans-cellular interactions mediate contact recognition and

56 signaling to promote synapse development. Moreover, this is the first study to test the effects of

57 disease-associated Kirrel3 missense variants on synapse formation, and thereby, provides a framework

58   to understand the etiology of complex neurodevelopmental disorders arising from rare missense

59   variants in synaptic genes.

60

61   **INTRODUCTION**

62   Autism spectrum disorder (ASD) has a strong genetic basis but the mechanistic links between

63   genetic risk variants and brain development remain poorly understood (Tick et al., 2016; Sandin et al.,

64   2017; Bai et al., 2019). This is likely because ASD patients have a heterogeneous set of atypical behaviors

65   presenting with a variety of co-morbid conditions and genetic variants in hundreds of genes are

66   identified as ASD risk factors (American Psychiatric Association, 2013; Rubeis et al., 2014; Iossifov et al.,

67   2014; Constantino and Charman, 2016). As such, it is important to understand how different types of

68   genetic risk variants functionally impact cells, circuits, and behavior to properly understand, diagnose,

69   and treat the diverse etiologies of individual patients (Geschwind and State, 2015).

70   Kirrel3 is an immunoglobulin (Ig)-domain containing transmembrane protein (Fig. 1A) that

71   undergoes homophilic trans-cellular binding (Sellin et al., 2002; Gerke et al, 2005; Martin et al., 2015).

72   Importantly, copy number variations and missense variants in Kirrel3 are repeatedly associated with

73   neurodevelopmental disorders including ASD and intellectual disability (ID) (Table 1) (Bhalla et al, 2008;

74   Kaminsky et al, 2011; Ben-David and Shifman, 2012; Guerin et al, 2012; Michaelson et al, 2012; Neale et

75   al, 2012; Talkowski et al, 2012; Iossifov et al, 2014; Rubeis et al, 2014; Wang et al, 2016; Yuen et al,

76   2016; Li et al, 2017; Guo et al, 2019; Leblond, et al, 2019). There are currently at least 17 missense

77   variants identified from multiple, independent studies lending credence to the possibility that altering

78   Kirrel3 function leads to ASD and ID. However, it remains unknown if Kirrel3 missense variants affect

79   protein function.

80   We recently discovered Kirrel3 is necessary for the formation of a specific type of synapse in the

81   rodent hippocampus (Martin et al., 2015; Martin et al., 2017). Here, dentate granule (DG) neurons

82   project axons, called mossy fibers, to area CA3 where they make unique excitatory synaptic complexes.

83   These mossy fiber synapse complexes connect DG neurons to CA3 neurons via giant presynaptic

84   boutons, each of which contains dozens of active zones capable of vesicle release (Acsady et al., 1998;

85   Bischofberger, 2006). Each giant presynaptic bouton also projects several presynaptic filopodia that, in

86   turn, build smaller excitatory synapses onto both CA3 neurons and GABAergic neurons in area CA3

87   (Acsády et al. 1998; Chicurel and Harris, 1992; Martin et al., 2017). In the hippocampus, Kirrel3 is only

88   detected in DG neurons and GABAergic neurons (Martin et al., 2015). Consequently, Kirrel3 knockout

89   animals have a highly specific loss of DG to GABAergic neuron mossy fiber filopodial synapses,

90   presumably via loss of trans-cellular contact recognition and downstream signaling mediated by Kirrel3

91   homophilic binding (Martin et al., 2015; Martin et al., 2017). Ultimately Kirrel3 loss-of-function leads to a

92   loss of feed-forward inhibition and an excitation/inhibition imbalance in the developing hippocampus

93   (Martin et al., 2015). In sum, previous work provides strong evidence that Kirrel3 is an important target-

94   specific, pro-synaptogenic molecule in vivo.

95   Several other recent studies also support a general role for Kirrel3 in mammalian

96   neurodevelopment. Specifically, Kirrel3 may also function at post-synapses in DG dendrites as DG

97   neurons from Kirrel3 knockout mice have more frequent miniature excitatory postsynaptic events in

98   young animals (Roh et al., 2017). Furthermore, Kirrel3 knockout mice have an array of aberrant

99   behavioral phenotypes, most notably characterized by hyperactivity, social, and communication deficits

100   (Choi et al., 2015; Hisaoka et al., 2018; Völker et al., 2018). Taken together, it is becoming clear that lack

101   of Kirrel3 function alters synapse development and adversely affects circuit function and behavior, but

102   the mechanisms underlying Kirrel3 function remain unknown.

103   Here, we sought to advance our understanding of Kirrel3 function and investigate how Kirrel3

104   variants could cause disease. To accomplish this, we developed a gain-of-function in vitro assay and

105   discovered that ectopic Kirrel3 expression specifically induces ectopic DG pre-synapse formation via

106   Kirrel3 homophilic interactions. We then tested the function of several disease-associated Kirrel3

107   missense variants identified in humans using the gain-of-function assay. We found that five out of six

108   disease-associated Kirrel3 variants tested have attenuated synaptogenic function. Intriguingly, we

109   identified two classes of non-functional variants: one that can neither mediate homophilic trans-cellular

110   interactions nor induce synapses, and one that can mediate homophilic trans-cellular interactions yet

111   has impaired synaptogenesis. We conclude that trans-cellular binding is necessary but not sufficient for

112   Kirrel3-mediated synapse formation and provide strong support that most disease-associated Kirrel3

113   variants impair Kirrel3 function and are bona fide risk factors for neurodevelopmental disorders.

114

115   **MATERIALS and METHODS**

116

117   Kirrel3 variant identification and cloning

118   Single nucleotide polymorphism (SNP) accession numbers for human disease-associated Kirrel3

119   missense variants are shown in Table 1 and were taken from the literature as indicated in the table and

120   the SFARI gene database (https://gene.sfari.org; Banerjee-Basu and Packer, 2010; Abrahams et al,

121   2013). The M673I variant is newly discovered and described below. Human Kirrel3 isoform 1

122   (NM_032531.4 nucleotide; NP_115920.1 protein) and mouse Kirrel3 Isoform A (NM_001190911.1

123   nucleotide; NP_001177840.1 protein) were aligned using Clustal Omega (Madeira et al., 2019) and

124   found to share 97.94% amino acid identity with identical length. Thus, all variants are named and

125   numbered according these isoforms. However, all experiments in this study use a cDNA encoding mouse

126   Kirrel3 isoform B (NM_026324.3 nucleotide; NP_080600.1) that is identical to isoform A except that it

127   lacks an alternatively spliced micro-exon encoding 12 amino acids near the transmembrane domain.

128   Isoform B contains all the conserved missense variant sites and was previously cloned by our lab with an

129   extracellular FLAG-tag in the vector pBOS (Martin et al., 2015). Variants were cloned using Q5 Site

130   Directed Mutagenesis (NEB Cat# E0554S) and QuikChangeII XL Site-Directed Mutagenesis (Agilent

131   Technologies Cat# 200521-5) kits. Mouse cDNA codon changes were made as follows: R40W (CGG to

132   TGG), R161H (CGG to CAT), R205Q (CGA to CAA), R336Q (CGA to CAA), M673I (ATG to ATT), and V731F

133   (GTC to TTC).

134

135   <u>Discovery of the Kirrel3 M673I variant</u>

136   We evaluated a 12 years old boy for ID, ADHD, and obesity. He is the only child of healthy

137   unrelated parents, born at term after an uneventful pregnancy; growth parameters at birth were normal

138   (height -0.5 SD, weight -0.5 SD and head circumference 0.5 SD). Neonatal hypotonia was noted. The

139   patient subsequently showed global developmental delay, with walking at 26 months and marked

140   language delay (first words at 4 years old). Neuropsychological evaluation at age 12 years showed

141   moderate intellectual disability. He is integrated in specialized schooling and cannot count or read. He

142   has fine motricity deficits. Moreover, he suffers from marked ADHD and benefits from methylphenidate

143   treatment. There are no autistic traits. Since 8 years of age, he has behavioral problems with frequent

144   oppositional crises. In addition, the parents report hyperphagia and food craving. At 12 years of age, his

145   height is at 0.5 SD, for a weight of + 3SD (BMI 25, with truncal obesity) and head circumference at -1.5

146   SD. The patient also presents with mild dysmorphic features, i.e. exophthalmos, bulbous nose with

147   slightly anteverted nares, thin upper lip and wide spaced teeth with two missing superior canines. Hands

148   are normal except for the presence of fetal pads; feet show 2-3rd toe syndactyly. There are no transit or

149   sleep issues. The boy had frequent otitis media during infancy, needing trans-tympanic drains; he is

150   wearing glasses for mild hypermetropia and astigmatism. Cerebral MRI at age 2 showed mild temporal

151   cortical atrophy and wide asymmetric aspect of posterior ventricular horns. Metabolic screening was

152   normal as well as karyotype, FMR1 gene analysis, 15q11.2 DNA methylation, and array-CGH.

153   Exome sequencing followed by targeted analysis of a panel of 990 genes implicated in intellectual

154   disability, identified a novel de novo missense variant in KIRREL3 c.2019G>A:p.(M673I) which was

155   classified as likely pathogenic according to the ACMG guidelines (Richards et al, 2015). This variant has

156   not been observed in gnomad V2.1.1

157   (https://gnomad.broadinstitute.org/gene/ENSG00000149571?dataset=gnomad_r2_1; 248436 alleles),

158   or gnomAD V3 (https://gnomad.broadinstitute.org/gene/ENSG00000149571?dataset=gnomad_r3;

159   143348 alleles), or the Bravo databases

160   (https://bravo.sph.umich.edu/freeze5/hg38/gene/ENSG00000149571; 125568 alleles) but a similar

161   variant, M673V, has been observed once in gnomAD V2.1.1, twice in gnomAD V3, and twice in Bravo.

162

163   Animals

164   Experiments involving animals were conducted in accordance with National Institute of Health

165   guidelines with approval from the University of Utah Institutional Animal Care and Use Committee.

166   Timed pregnant Sprague Dawley dams were ordered from Charles River (Strain Code 400; RRID:

167   RGD_737926). Wild-type C57BL/6J mice (RRID: IMSR_JAX:000664) were originally obtained from The

168   Jackson Laboratory. Generation of Kirrel3 knockout mice was previously reported (Prince et al., 2013).

169   Knockouts were maintained in a C57BL/6J background. Hippocampi from male and female newborn (P0)

170   pups were combined for neuron cultures.

171

172   Immunostaining

173   Cells on glass coverslips were fixed at room temperature for 10-15 minutes in 4% PFA made in

174   PBS. Cells were rinsed two times with PBS and blocked/permeabilized in PBS with 3% BSA and 0.1%

175   Triton-x for 30 minutes. Cells were incubated with primary antibodies diluted in PBS with 3% BSA for 1-2

176   hours at room temperature with rocking, rinsed three times in PBS with 3% BSA and incubated with

177 secondary antibodies diluted in PBS with 3% BSA for 45 minutes. After rinsing, coverslips were mounted

178 in Fluoromount-G (Southern Biotech Cat# 0100-01). For surface labelling, live neurons were incubated in

179 serum-free media at 37˚C in a 5% CO_2 incubator with chicken-anti-FLAG for 20 minutes. After initial

180 incubation, neurons were fixed, permeabilized and stained as above.

181

182 Antibodies

183   Primary antibodies used include: rabbit-anti-Fox1 (1:3600, Abcam, Cat# ab16645, RRID:

184 AB_732428), guinea pig-anti-VGluT1 (1:5000, Millipore, Cat# AB5905, RRID: AB_2301751), goat-anti-

185 synaptoporin (SPO, 1:1000, Santa Cruz Biotechnology, Cat# sc-51212, RRID: AB_ 1129844), goat-anti-

186 GFP (1:3000, Abcam, Cat# ab6673, RRID: AB_305643), mouse-anti-PSD-95 (1:1000, Neuromab, Cat# 75-

187 348, RRID: AB_2315909), chicken-anti-FLAG (1:1000, Gallus Immunotech, Cat# AFLAG), mouse-anti-FLAG

188 M2 (1:5000, Sigma, Cat# F1804, RRID: AB_262044), mouse anti-FLAG M2-Cy3 conjugated (1:1000,

189 Sigma, Cat# A9594, RRID: AB_ 439700), rabbit-anti-2A (1:1000, Millipore, Cat# ABS31, RRID:

190 AB_11214282).

191   Secondary antibodies were all all used at 1:1000 and include: donkey-anti-rabbit-Alexa 488

192 (Invitrogen, Cat# A21206, RRID: AB141708), donkey-anti-rabbit-Cy3 (Jackson ImmunoResearch, Cat#

193 711-165-152, RRID: AB_2307443), donkey-anti-guinea pig-Alexa 647 (Jackson ImmunoResearch, Cat#

194 705-605-147, RRID: AB_2340437), donkey-anti-guinea pig-DyLight 405 (Jackson ImmunoResearch, Cat#

195 706-475-148, RRID: AB_2340470), donkey-anti-goat-Cy3 (Jackson ImmunoResearch, Cat# 705-165-147,

196 RRID: AB_2307351), donkey-anti-goat-Alexa 647 (Jackson ImmunoResearch, Cat# 705-605-147, RRID:

197 AB_2340437), donkey-anti-goat-Alexa 488 (Jackson ImmunoResearch, Cat# 705-545-147, RRID:

198 AB_2336933), donkey-anti-mouse-Cy3 (Jackson ImmunoResearch, Cat# 715-165-150,

199 RRID:AB_2340813), donkey-anti-mouse-Alexa 647 (Jackson ImmunoResearch, Cat# 715-605-150, RRID:

200 AB_2340862), donkey-anti-mouse-Alexa 488 (Invitrogen, Cat# A21202, RRID: AB_141607), donkey-anti-

201   chicken-Alexa 647 (Jackson ImmunoResearch, Cat# 703-605-155, RRID: AB_2340379), donkey-anti-

202   chicken-Cy3 (Jackson ImmunoResearch, Cat# 703-165-155, RRID: AB_2340363).

203

204   <u>Neuron culture</u>

205   Neuron cultures were prepared as previously described (Martin et al., 2015; Basu et al., 2017).

206   Briefly, rat cortical astrocytes were plated to glass coverslips coated with 0.03mg/ml ($\sim$7.5μg/cm^2) of

207   PureCol (Advanced Biomatrix, Cat# 5005) and grown to confluence in glia feeding media: MEM (GIBCO

208   Cat# 11090-081) supplemented with 10% FBS (Atlas Biologicals Cat# FP-0500-A), 30mM glucose, 1x

209   penicillin-streptomycin solution (GIBCO Cat# 15070-063). P0 mouse or rat hippocampi were dissected in

210   ice cold Hank's Balanced Salt Solution (HBSS; Cat# GIBCO 14185-052) supplemented with 2.5mM HEPES

211   pH7.4, 30mM glucose, 1mM $CaCl_2$, 1mM $MgSO_4$ and 4mM $NaHCO_3$. Hippocampi were dissociated by

212   incubating in papain solution (20 units/ml papain (Worthington Cat# 3126), 82mM Na_2SO_4, 30mM K_2SO_4,

213   5.8mM $MgCl_2$, 0.25mM $CaCl_2$, 1mM HEPES pH 7.4, 20mM glucose and 0.2mM NaOH) for 30 minutes at

214   37˚C followed by trituration through a polished glass pipette. Dissociated cells were rinsed and

215   resuspended in neuron plating media: MEM supplemented with 10% horse serum (LifeTechnologies

216   Cat# 26050-088), 20mM glucose, 1x penicillin-streptomycin solution, 2mM Glutamax (GIBCO Cat#

217   35050-061), and 1mM sodium pyruvate. Dissociated hippocampal cells were electroporated with 1 pulse

218   at 340V for 900μs pulse length using a square wave protocol in a cuvette with a 2mm electrode (BTX,

219   ECM830, Harvard Apparatus Cat# 45-0002) using the appropriate plasmids and plated at 1x10^5 cells/well

220   onto glia coated coverslips in a standard 12-well plate. Neurons were kept in a 37˚C incubator

221   maintained with 5% CO_2. A few hours after plating, the neuron plating media was replaced with

222   hippocampal feeding media: Neurobasal A (GIBCO Cat# 10888-022) supplemented with 1x B-27 (GIBCO

223   Cat# 17504-044), 0.2x penicillin-streptomycin solution, 0.5mM Glutamax, 12mM glucose and 1μM AraC

224   (Sigma-Aldrich Cat# C6645).

225

226   Gain-of-function synapse induction assay

227   Neurons were transfected with GFP-pBOS or co-transfected with GFP-pBOS + FLAG-Kirrel3-pBOS

228   constructs. Equal amounts of DNA were transfected for each condition. Cultures were harvested at 14

229   days in vitro (DIV) and stained with mouse-anti-GFP, rabbit-anti-Foxp1, guinea pig-anti-VGluT1 and goat-

230   anti-synaptoporin. Transfected CA1 neurons, identified by GFP expression, strong expression of the

231   marker Foxp1 and pyramidal morphology, were imaged at 63x magnification on a Zeiss LSM-7 confocal

232   microscope. Maximum intensity projected images were analyzed in ImageJ. The number of VGluT1 only

233   (originating predominantly from principle excitatory neurons of the CA3, CA2 and CA1 fields combined),

234   SPO only (originating from interneurons) and VGluT1 + SPO co-labelled puncta (originating from DG

235   neurons) were counted along CA1 dendrites and the density was calculated as the number of puncta per

236   length of dendrite. Analysis was performed blind to condition.

237

238   Neuron/HEK293 co-culture assays

239   Neuron-HEK293 co-cultures were prepared according to an established method (Biederer and

240   Scheiffele, 2007). Briefly, P0 rat hippocampal neurons were plated to poly-D-lysine (PDL; $10\mu g/cm^2$;

241   Millipore Cat# A-003-E) coated coverslips at $5x10^4$ neurons per well in a 24-well plate. HEK293T cells

242   (ATCC Cat# CRL-3216; RRID: CVCL_0063) were transfected with either GFP-pBOS, GFP-pBOS + FLAG-

243   Neuroligin-1 pCDNA, GFP-pBOS + FLAG-Neurexin-1β-AS4(-)-pCDNA or GFP-pBOS + FLAG-Kirrel3-pBOS

244   (wild-type) 24 hours before seeding to neurons. In one condition for the presynaptic assay, the neurons

245   were electroporated with FLAG-Kirrel3-pBOS before plating.

246   Test for pre-synapse induction: Transfected HEK293 cells were seeded to 6 DIV neurons at $3x10^4$

247   cells per well. 24 hours later co-cultures were fixed and immunostained with mouse-anti-FLAG, guinea

248   pig-anti-VGluT1 and goat-anti-GFP. Transfected HEK293 cells in proximity to VGluT1 positive axons were

249   imaged and analyzed. To determine the presynaptic hemisynapse density, the total area of VGluT1

250   puncta on or within 0.5μm of the edge of each HEK293 cell was quantified and normalized to the total

251   area of the cell in ImageJ. Analysis was performed blind to condition.

252   Test for post-synapse induction: Transfected HEK293 cells were seeded to 14 DIV neurons at

253    $3x10^4$ cells per well. 24 hours later co-cultures were fixed and immunostained with mouse-anti-FLAG,

254   guinea pig-anti-VGluT1, mouse-anti-PSD-95 and goat-anti-GFP. HEK293 cells in proximity to PSD-95

255   positive dendrites were imaged and analyzed. To determine the postsynaptic hemisynapse density, the

256   total area of PSD-95 positive, VGluT1 negative puncta on or within 0.5μm of the edge of each HEK293

257   was quantified and normalized to the total area of the cell in ImageJ. Analysis was performed blind to

258   condition.

259

260   <u>Axon contact assay</u>

261   P0 Kirrel3 knockout neurons were dissociated and transfected for two conditions. For condition

262   1 (Kirrel3 cells plus control cells): $2.5x10^4$ neurons per well were co-transfected with GFP-pBOS + FLAG-

263   Kirrel3-pBOS and another $2.5x10^4$ neurons per well were transfected with mCherry-pBOS. For condition

264   2 (Kirrel3 cells plus Kirrel3 cells): $2.5x10^4$ of the neurons per well were co-transfected with GFP-pBOS +

265   FLAG-Kirrel3-pBOS and $2.5x10^4$ neurons per well were co-transfected with mCherry-pBOS + FLAG-

266   Kirrel3-pBOS. In both conditions, transfected neurons were plated with $5x10^4$ untransfected neurons per

267   well. Neurons were fixed at 7 DIV. GFP-positive dendrites contacting mCherry-positive axons were

268   imaged at 63x and analyzed in ImageJ. To compare the relative amount of mCherry positive axon

269   contact with GFP positive neurons between the conditions, we defined an axon contact index. We

270   created a GFP-positive cell mask by thresholding the GFP channel and an axon mask by thresholding the

271   mCherry channel. The area of mCherry axon mask within in the GFP cell mask was measured. Analysis

272   was performed blind to condition.

273

Synapse localization assay

275   P0 rat hippocampi were dissociated and electroporated with wild-type mCherry-2A-FLAG-

276   Kirrel3-pBOS, or the missense variants, and cultured as described above. At 21 DIV, neurons were live-

277   labelled with chicken-anti-FLAG, fixed, and immunostained with rabbit-anti-2A, guinea pig-anti-VGluT1

278   and mouse-anti-PSD-95. mCherry-expressing neurons were imaged at 63x and analyzed in ImageJ.

279   Synapses were determined by the juxtaposition of VGluT1 and PSD-95 puncta. The number of synapses

280   was quantified along the dendrites and scored as either FLAG-Kirrel3 positive or FLAG-Kirrel3 negative to

281   determine the percent of synapses with FLAG-Kirrel3. Analysis was performed blind to condition.

282

Surface expression assay

284   Chinese hamster ovarian-K1 (CHO) cells (ATCC, Cat# CCL-61, RRID: CVCL_0214) were plated on

285   PDL-coated (10μg/cm^2), 18mm coverslips in a 12-well plate at 1x10^5 cells per well. 24 hours later, cells

286   were transfected with GFP-pBOS or GFP-pBOS + FLAG-Kirrel3-pBOS constructs. Another 24 hours later,

287   cells were live-labelled with chicken-anti-FLAG before permeabilization to detect surface expressed

288   FLAG-Kirrel3. Cells were then fixed, permeabilized and stained with mouse-anti-FLAG to detect

289   intracellular Kirrel3 along with goat-anti-GFP to label transfected cells. The integrated density of the

290   chicken-anti-FLAG (extracellular) signal was quantified per cell and divided by the integrated density of

291   the mouse-anti-FLAG (intracellular) signal to determine the extracellular/intracellular ratio. General

292   culture conditions and solutions for CHO cells were previously described (Martin et al., 2015; Basu et al.,

293   2017). Analysis was performed blind to condition.

294

Cell aggregation assay

296   The aggregation assay was performed as previously described (Martin et al., 2015; Basu et al.,

297   2017). CHO cells were transfected with mCherry-pBOS, wild-type mCherry-2A-FLAG-Kirrel3-pBOS, or the

298   missense equivalents. The aggregation index was calculated by dividing the mCherry integrated density

299   in aggregated cell clumps by the total mCherry integrated density in the well. Analysis was performed

300   blind to condition.

301

302   Immunoblotting

303   Immunoblotting was conducted by standard techniques. Briefly, CHO cells or HEK293 cells were

304   transfected as needed in a 12-well plate. Cells were collected in 400µL of Laemmli buffer, boiled, run on

305   a 10% Tris-glycine gel, and transferred to a nitrocellulose membrane. The membrane was probed with

306   mouse-anti-Kirrel3 (Neuromab, Cat# 75-333, RRID: AB_2315857) and mouse-anti-GAPDH (Millipore,

307   Cat# AB2302, RRID: AB_ 10615768). Secondary antibody was goat-anti-mouse-HRP (Jackson

308   ImmunoResearch, Cat# 115-035-003, RRID: AB_10015289).

309

310   Experimental Design and Statistical Analysis

311   Sample sizes were estimated a priori based on results from previous studies (Williams et al,

312   2011; Martin et al., 2015; Basu et al., 2017). Statistics were computed using Graphpad Prism (RRID:

313   SCR_002798). All data were tested for normality using a D'Agostino and Pearson omnibus normality test

314   and then appropriate parametric or non-parametric tests were used and are reported in the results. For

315   all multiple comparisons, we report the multiplicity adjusted p-values. Graphs show mean +/- SEM. A p-

316   value < 0.05 was considered significant for all tests. *p<0.05, **p<0.01 ***p<0.001, ****p<0.0001. Data

317   from separate experimental trials were normalized to the negative control for the experimental trial

318   before combining datasets to control for culture to culture variability. For k-means clustering we used

319   the mean rank values for each condition from the synapse induction assay and the cell aggregation assay

320   consistent with the non-parametric tests used to compare them. Mean ranks were normalized to the

321   wild-type mean rank for ease of viewing.

322

323   **RESULTS**

324

325   Exogenous Kirrel3 expression induces ectopic synapse formation between incorrect targets

326   Kirrel3 knockout results in selective synapse loss but it is unknown if Kirrel3 plays an instructive

327   role in selective synapse development. To complement our previous loss-of-function studies, we sought

328   to test if exogenous Kirrel3 expression induces synapse formation via a gain-of-function assay. To this

329   end, we developed an in vitro assay based on the fact that target specific synapse formation is largely

330   maintained between cultured hippocampal neurons (Williams et al., 2011). Previously it was shown that

331   cultured DG neurons frequently synapse with CA3 neurons (an appropriate target in vivo) but only rarely

332   synapse with CA1 neurons (an inappropriate target in vivo) despite the fact that DG axons similarly

333   contact CA3 and CA1 dendrites in culture (Williams et al., 2011). Because CA1 neurons do not

334   appreciably express Kirrel3, we used this in vitro specificity to our advantage and tested if exogenous

335   Kirrel3 expression in CA1 neurons could induce ectopic DG-to-CA1 synapses (Fig. 1B).

336   To accomplish our goal, we needed to unambiguously identify CA1 neurons and DG synapses in

337   culture. We demonstrate that CA1 neurons are identified by high expression of the transcription factor

338   Foxp1, while pre-synapses arising from DG axons are identified by co-expression of the presynaptic

339   proteins synaptoporin (SPO) and vesicular glutamate transporter 1 (VGluT1) (Fig. 1C; Ferland et al.,

340   2003; Williams et al., 2011;). This combination of markers allows us to quantify the number of DG pre-

341   synapses formed onto CA1 dendrites. We transfected dissociated rat hippocampal neurons with GFP

342   alone or GFP plus FLAG-Kirrel3 and quantified the number of DG pre-synapses per unit length of CA1

343   dendrite to determine the DG pre-synapse density in GFP-positive neurons (Fig. 1D-E). Normally,

344   cultured CA1 neurons have few DG pre-synapses but exogenous expression of Kirrel3 in CA1 neurons

345   significantly increases the density of DG pre-synapses onto CA1 neurons by more than two-fold (Fig. 1E;

346   Mann-Whitney U=570, p=0.0027). This effect is specific for DG synapses as we do not observe an

347   increase in the number of synapses arising from other types of glutamatergic neurons in the culture.

348   This includes CA3, CA2, and CA1 neurons, which are collectively marked by expression of VGluT1, but

349   not synaptoporin, and are referred to here as CA synapses (Fig. 1F; Mann-Whitney U=905, p=0.9552).

350   Kirrel3 mediates homophilic, trans-cellular adhesion in vitro, and in vivo loss of function studies

351   suggest that Kirrel3 mediates synapse formation selectively between Kirrel3-expressing neurons (Gerke

352   et al, 2005; Serizawa et al, 2006; Martin et al., 2015). Together, this suggests Kirrel3's function requires

353   trans-cellular interactions with other Kirrel3 molecules. Since all DG neurons normally express Kirrel3,

354   we next tested if Kirrel3's gain-of-function effect depends upon the presence of endogenous Kirrel3 in

355   DG axons. To do this, we performed the same assay in hippocampal neurons cultured from both Kirrel3

356   wild-type and knockout mice, taking extra precaution to not quantify CA1 neurons that were contacted

357   by transfected axons (marked by GFP). Similar to our results in rat neurons, we find that exogenous

358   Kirrel3 expression potently induces ectopic DG-to-CA1 synapses in cultures prepared from wild-type

359   mice, but Kirrel3 has no synaptogenic activity in cultures prepared from Kirrel3 knockout mice (Fig. 1G;

360   two-way ANOVA, $F_{(1,111)}$=5.049, interaction, p=0.0266; Sidak's multiple comparison WT-GFP vs WT-

361   Kirrel3 p=0.0088, KO-GFP vs KO-Kirrel3 p=0.9560). This strongly suggests that in our gain-of-function

362   assay postsynaptic Kirrel3 in the CA1 dendrite interacts with pre-synaptic Kirrel3 in the DG axons to

363   induce synapse formation via homophilic, trans-cellular interactions (Fig. 1H).

364

365   Kirrel3-induced synapses do not result from increased axon-dendrite contact

366   It is possible Kirrel3 interactions directly instruct neurons to recruit synaptic components at

367   existing axon-dendrite contact points. Alternatively, Kirrel3 expression may increase the amount of

368   axon-dendrite contact between DG and CA1 neurons, and thereby increase the chance that synapses

369   will form via other molecules. Thus, we next tested if Kirrel3 expression increases axon-dendrite

370   contacts. Tools to identify endogenously-expressing Kirrel3 positive and negative axons in culture are

371   not available, so we cultured neurons from Kirrel3 knockout mice and transfected Kirrel3 in a controlled

372   manner. Knockout neurons were co-transfected with GFP and Kirrel3 and mixed with knockout neurons

373   transfected with either mCherry, or mCherry and Kirrel3. Thus, while in both conditions GFP-labelled

374   neurons expressed Kirrel3: in one condition they were contacted by mCherry axons that were Kirrel3

375   negative, and in the other condition they were contacted by mCherry axons that were Kirrel3 positive.

376   Quantification of the overlap between GFP dendrites and mCherry axons revealed a similar amount of

377   axon-dendrite overlap regardless of whether the axons expressed Kirrel3 or not (Fig. 2A-2B; Mann-

378   Whitney U=257, p=0.2445). This suggests Kirrel3 expression does not induce synapses simply by

379   increasing axon-dendrite contact and supports a model in which Kirrel3 trans-cellular interactions

380   actively recruit synaptic factors to existing points of axon-dendrite contacts.

381

382   Kirrel3-mediated synaptogenesis requires post-synaptic neurons

383   We next tested if Kirrel3 is sufficient to induce synapses using a well-established co-culture

384   assay in which synaptogenic proteins are presented to neurons in non-neuronal cells (Scheiffele et al.

385   2000, Graf et al., 2004; Biederer and Scheiffele, 2007). In this assay, neurons abundantly contact HEK293

386   cells but do not recognize HEK293 cells as synaptic partners. However, if HEK293 cells express some

387   postsynaptic molecules such as Neuroligin-1, the neurons form presynapse structures, identified by

388   VGlut1, on the HEK293 cells (Fig. 3A) (Scheiffele et al., 2000). Conversely, when HEK293 cells express

389   some presynaptic molecules such as Neurexin-1, the neurons form postsynapse structures, identified by

390   PSD-95, on the HEK293 cells (Graf et al., 2004). Interestingly, we find that when HEK293 cells express

391   Kirrel3, the neurons form neither pre- nor post-synapses with HEK293 cells, though both of our positive

392   controls (Neurexin-1 and Neuroligin-1) functioned as expected (Fig. 3A-3D; Pre-synapses: Kruskal-Wallis

393   test with Dunn's multiple comparisons GFP vs Kirrel3 p=0.3988, GFP vs Neuroligin-1 p=0.0074; Post-

394   synapses: Kruskal-Wallis test with Dunn's multiple comparisons GFP vs Kirrel3 p>0.9999, GFP vs

395   Neurexin-1 p=0.0252). Because Kirrel3 expression specifically induces DG synapses, we also conducted

396   this assay using the DG-specific marker synaptoporin instead of the generic marker VGluT1.

397   Unfortunately, we find synaptoporin is not reliably expressed in the 7 DIV neurons used for this assay.

398   We circumvented this limitation by transfecting extra Kirrel3 into hippocampal neurons and then

399   quantifying the density of presynaptic puncta on Kirrel3-expressing HEK293 cells contacting Kirrel3-

400   transfected axons. We found that this still had no effect on the density of pre-synapses formed onto

401   HEK293 cells (Fig. 3A-B; Kruskal-Wallis test with Dunn's multiple comparisons GFP vs Kirrel3 neuron and

402   HEK293 expression p>0.9999). In conclusion, we find Kirrel3 is not sufficient to induce synapses when

403   expressed in a non-neuronal cell. Taken together, our work indicates that Kirrel3's synaptogenic function

404   requires both trans-cellular Kirrel3 binding and interactions with an additional co-factor(s) present in

405   CA1 neurons but not in HEK293 cells.

406

407   Kirrel3 missense variants appropriately traffic to synapses and the cell surface

408   Thus far, we used our in vitro gain-of-function assay to identify basic mechanistic principles of

409   Kirrel3 signaling during synapse formation. Next, we tested if and how disease-associated Kirrel3

410   missense variants affect its function. Accordingly, we cloned six missense variants identified as possible

411   risk factors for neurodevelopmental disorders (Fig. 4A; Table 1; Bhalla, et al., 2008; De Rubeis, et al.,

412   2014; Iossifov, et al., 2014; Yuen, et al., 2016). These variants span the length of the Kirrel3 protein and

413   are fully conserved between the mouse and human proteins, which share 98% amino acid identity

414   (Gerke et al., 2005). Most variants are found in patients with both autism and intellectual disability. One

415   variant, M673I, has not been reported previously. We identified this as a likely pathogenic variant in a

416   male patient with developmental delay, intellectual disability, ADHD, and obesity (see methods for

417   complete description).

418   Missense variants can impair the function of synaptic molecules by altering their trafficking or

419   surface expression (Chih et al., 2004; Zhang et al., 2009; Jaco et al., 2010). Thus, we first tested if Kirrel3

420   variants are expressed on the cell surface similar to wild-type Kirrel3. We transfected CHO cells with

421   Kirrel3 plasmids containing an extracellular FLAG tag that does not interfere with Kirrel3 homophilic

422   binding (Martin et al., 2015). The cells were live-labelled with chicken-anti-FLAG antibodies to label

423   Kirrel3 protein on the extracellular surface. Then, cells were fixed, permeabilized, and incubated with

424   mouse-anti-FLAG antibodies to label intracellular Kirrel3 (Fig. 4B). The ratio of extracellular to

425   intracellular Kirrel3 was quantified for individual cells. We find the relative intensities of extracellular to

426   intracellular FLAG-Kirrel3 are indistinguishable between groups, indicating that all six missense variants

427   are appropriately trafficked to the cell surface similar to wild-type Kirrel3 (Fig. 4C; one-way ANOVA

428     $F_{(6,56)}$=0.9878, p=0.4424).

429   Wild-type Kirrel3 localizes at or near excitatory synapses (Martin et al., 2015; Roh et al, 2017).

430   Thus, we tested if Kirrel3 missense variants also localize to the cell surface at synapses in neurons. We

431   expressed mCherry-2A-FLAG Kirrel3 and missense variants in cultured neurons and determined their

432   localization relative to synapses by co-staining for surface-expressed FLAG, VGluT1, and PSD-95 (Fig. 4D).

433   All Kirrel3 variants display a punctate expression pattern and are found in close proximity to juxtaposed

434   VGluT1/PSD-95 puncta at similar rates (Fig. 4E; Kruskal-Wallis test =7.013; p=0.3197). Collectively, we do

435   not observe general trafficking defects in disease-associated Kirrel3 missense variants.

436

437   Disease-associated Kirrel3 variants attenuate Kirrel3 function

438   We next tested the ability of each variant to induce DG pre-synapses when ectopically expressed

439   in CA1 neurons compared to wild-type (as shown Figure 1D). Importantly, we found that four of the six

440   disease-associated variants (R161H, R205Q, R336Q and V731F) significantly attenuate Kirrel3 mediated

441   pre-synapse formation when compared to wild-type Kirrel3 (Fig. 5A-B, Kruskal-Wallis test with Dunn's

442   multiple comparisons WT vs GFP p=0.<0.0001, WT vs R40W p=0.2495, WT vs R161H p=0.0472, WT vs

443   R205Q p=0.0218, WT vs R336Q p=0.0135, WT vs M673I p=0.9844, WT vs V731F p=0.0032). Another

444   variant, R40W, appears to attenuate synapse formation but does not achieve statistical significance in

445   this comparison. We then applied statistical tests to determine the ability of the missense variants to

446   induce pre-synapse formation relative to negative control neurons transfected with GFP alone using the

447   same dataset. Consistent with our previous analysis, DG-pre-synapse densities on CA1s expressing

448   R161H, R205Q, R336Q or V731F are not significantly different from GFP-only transfected neurons,

449   suggesting that these variants do not induce synapse formation (Fig. 5C; Kruskal-Wallis test with Dunn's

450   multiple comparisons GFP vs WT p<0.0001, GFP vs R161H p>0.9999, GFP vs R205Q p>0.9999, GFP vs

451   R336Q p>0.9999, GFP vs M673I p=0.0382, GFP vs V731F p>0.9999). In addition, we found that the R40W

452   variant is also not significantly different from GFP transfected controls (Kruskal-Wallis test with Dunn's

453   multiple comparisons GFP vs R40W p=0.1299), suggesting that this variant also does not induce synapse

454   formation. The different outcomes for this variant depending on the statistics applied suggest that the

455   R40W variant likely attenuates Kirrel3 function very near the sensitivity threshold of this functional

456   assay. Thus, we conclude that five of the six tested disease-associated Kirrel3 variants have impaired

457   synaptogenic function. Our results provide the first functional evidence that Kirrel3 missense variants

458   may cause disease through the selective loss of synapses.

459

460   Kirrel3 missense variants fail to induce pre-synapses via different mechanisms

461   Missense variants affecting Kirrel3 function span the extracellular and intracellular domains

462   suggesting they may impair Kirrel3 function in distinct ways (Fig. 4A, Table 1). We reasoned that variants

463   in the extracellular domain may eliminate Kirrel3 homophilic binding while variants in the intracellular

464   domain may alter downstream signaling. It is not yet possible to test Kirrel3 intracellular signaling

465   because very little is known about Kirrel3's intracellular interactions or signaling mechanisms. Therefore,

466   we tested the ability of each missense variant to mediate homophilic binding in trans using an

467   established CHO cell aggregation assay. CHO cells do not endogenously express appreciable levels of

468   Kirrel3 (Fig. 6A) and when mixed in suspension they do not normally form cell aggregates (Fig. 6B-C). In

469   contrast, CHO cells transfected with wild-type Kirrel3 form multicellular aggregates consistent with

470   Kirrel3 undergoing homophilic, trans-cellular binding (Fig. 6B-C; Martin et al., 2015). After testing each

471   variant, we find that cells transfected with R40W, R161H, R336Q and M673I aggregate similarly to wild-

472   type Kirrel3, but the R205Q and V731F missense variants do not induce cell aggregation (Fig. 6C, Kruskal-

473   Wallis test with Dunn's multiple comparisons WT vs Ctrl p<0.0001, WT vs R40W p>0.9999, WT vs R161H

474   p>0.9999, WT vs R205Q p<0.0001, WT vs R336Q p>0.9999, WT vs M673I p>0.9999, WT vs V731F

475   p=0.0042). Subsequent k-means clustering defines four groups of variants with respect to synaptogenic

476   and aggregation ability (Fig. 6D). Wild-type Kirrel3 and the M673I variant group together as they exhibit

477   homophilic trans-cellular binding and induce synapse formation to a greater extent than the other

478   variants. The R40W variant is isolated reflecting its intermediate ability to induce synapse formation

479   with normal trans-cellular binding. R161H and R336Q form a group characterized by attenuated

480   synaptogenic ability with normal trans-cellular binding. Finally, R205Q and V731F group with the

481   negative control as they are completely binding deficient and do not induce synapse formation.

482   Collectively these results indicate that missense variants impact Kirrel3 function in distinct ways: some

483   attenuate Kirrel3 mediated trans-cellular interactions, while others maintain an ability to mediate

484   contact recognition but still fail to induce synaptogenesis strongly implicating additional unidentified

485   signaling mechanisms.

486

487   **DISCUSSION**

488   Kirrel3 functions in synapse development as a homophilic cell-recognition tag

489   Most synapses do not form randomly between any neurons that come into contact with each

490   other. Rather, neurites coursing through a dense microenvironment often select specific partners

491   among a milieu of incorrect choices. A long-standing hypothesis proposes that neuronal wiring requires

492   matching affinity tags selectively expressed on pre- and postsynaptic neurons (Sperry, 1963; Benson et

493   al., 2001; Sanes and Yamagata, 2009; Südholf, 2018). The identity of these tags and how they signal at

494   specific synapses remain largely unresolved.

495   Here, we directly tested if Kirrel3 acts as synaptogenic, cell-recognition tag using a novel gain-of-

496   function assay. We demonstrate that ectopic Kirrel3 expression in CA1 neurons specifically induces

497   ectopic DG synapse formation, providing the first direct evidence that Kirrel3 plays an instructive role in

498   synapse development. Furthermore, we show that ectopic Kirrel3 has no function when expressed in

499   cultures prepared from Kirrel3 knockout mice. This indicates that ectopically-expressed Kirrel3 function

500   depends on the presence of endogenous Kirrel3, most likely because ectopic Kirrel3 in the CA1 dendrites

501   interacts with endogenous Kirrel3 in DG axons to induce DG synapses. This strongly suggests Kirrel3's

502   trans-cellular, homophilic interactions are necessary for its function. This is significant because, although

503   prior work indicates that Kirrel3 can undergo homophilic interactions, a functional role of Kirrel3

504   homophilic interactions at synapses had not been directly tested (Gerk et al., 2005; Serizawa et al.,

505   2006; Martin et al., 2015; Prince et al., 2013; Brignall et al., 2018). Moreover, in the mouse

506   neuromuscular junction, mouse kidney, and at C. elegans synapses, Kirrel3 functions via heterophilic

507   interactions with another Ig-superfamily protein Nephrin-1 (C. elegans Syg-1, Syg-2 respectively) (Shen

508   and Bargmann, 2003; Shen et al., 2004; Gerke et al., 2005; Ding et al., 2007; Chao et al., 2008; Komori et

509   al., 2008; Chia et al., 2014; Özkan et al., 2014). Our study does not rule out the possibility that Kirrel3

510   binds in trans to other molecules, but we clearly show that Kirrel3-Kirrel3 trans-homophilic interactions

511   are necessary for its synaptogenic function.

512

513 <u>Kirrel3 has multifaceted roles as a recognition, adhesion, and signaling molecule</u>

514   Cell adhesion proteins are important for contact recognition between neurons but very little is

515 known about downstream signaling events that couple contact recognition to synapse development.

516 Therefore, a common misperception is that adhesive proteins expressed on the cell surface act as a

517 "molecular glue" to hold juxtaposed membranes together long enough for other general synaptogenic

518 factors to be recruited. In contrast, our findings support a model in which Kirrel3 likely mediates a

519 combination of contact recognition, adhesion, and downstream synaptogenic signaling and directly

520 implicate Kirrel3 as a bona fide signaling molecule. Several lines of evidence support this conclusion.

521 First, in support that Kirrel3 likely mediates contact recognition and adhesion, we identified two

522 variants, R205Q and V731F, that cannot bind in trans and have no synaptogenic activity. This supports

523 the conclusion that trans-cellular binding is necessary for Kirrel3 function. Interestingly, the V731F

524 variant resides in the Kirrel3 intracellular domain and we speculate that this variant produces a

525 conformational change that directly inhibits trans-cellular interactions by the extracellular domain.

526 Nonetheless, our results strongly suggest that trans-cellular binding is absolutely critical for Kirrel3

527 synaptic function. Second, in support of the idea that Kirrel3 has a non-adhesive signaling function, we

528 also identified variants, R161H and R336Q, which bind normally in trans yet have impaired synaptogenic

529 activity. These results indicate that trans-cellular binding is not sufficient for Kirrel3 function and

530 strongly suggest Kirrel3 is involved in synaptic signaling in addition to its role in trans-cellular recognition

531 or adhesion. Additional support for this conclusion comes from the fact that Kirrel3 is not synaptogenic

532 if presented to neurons by a non-neuronal cell. This also strongly suggests that trans-cellular binding is

533 not sufficient for its synaptogenic function and that Kirrel3 function requires a neuronal co-factor. In

534 sum, we find that trans-cellular binding is necessary but not sufficient for Kirrel3 function and that

535   Kirrel3 must interact with other neuronal proteins to induce a synapse. Thus, Kirrel3 does more than act

536   as synaptic glue.

537

538   <u>What proteins might mediate a Kirrel3 signal?</u>

539   For the presynaptic DG axon to differentiate between a HEK293 cell and neuron, we postulate

540   that Kirrel3 likely interacts with another extracellular or transmembrane molecule in the postsynaptic

541   neuron and that molecule must be lacking in the HEK293 cell. Interestingly, the Kirrel3 extracellular

542   domain was reported to interact with the cell adhesion molecule Neurofascin but this remains to be

543   tested under physiological conditions (Völker et al., 2018).

544   Kirrel3 intracellular interactions are also likely to be important for Kirrel3 mediated synapse

545   development. Most interestingly, the Kirrel3 intracellular domain ends in a conserved PDZ-binding

546   domain, which is a common protein motif of synaptic organizing molecules. It was suggested that mouse

547   Kirrel3 binds to the PDZ domain proteins CASK, PSD95, and ZO-1 (Huber et al., 2003; Gerke et al., 2006;

548   Roh et al., 2017). Other evidence for putative Kirrel3 binding partners comes from studies using

549   Drosophila and C. elegans. Here, Kirrel3 orthologues are shown to physically or genetically interact with

550   Rols7 (Tanc1/2, a synaptic scaffold), Loner (Brag2, an Arf-GEF), Lin10 (Mint, an active zone component),

551   WVE-1 (WAVE-1, an actin regulator), and SKR-1 (Skp1, an E3 ubiquitin ligase) (Kreisköther et al., 2006;

552   Vishnu et al., 2006; Bulchand et al., 2010; Ding et al., 2007; Chia et al., 2014). However, none of these

553   Kirrel3 interacting proteins have yet been well validated under physiological conditions in the

554   mammalian brain. Further work is needed to identify new Kirrel3 signal transduction candidates and

555   screen existing candidates. The identity of Kirrel3 signaling molecules and whether or not they are

556   shared by other synapse specificity factors will be an important question to address in future studies.

557

558   <u>Kirrel3 variants associated with disease impair synapse formation</u>

559   Kirrel3 is an emerging hotspot for rare variants linked to neurodevelopmental disorders (Bhalla

560   et al, 2008; Kaminsky et al, 2011; Ben-David and Shifman, 2012; Guerin et al, 2012; Michaelson et al,

561   2012; Neale et al, 2012; Talkowski et al, 2012; Iossifov et al, 2014; Rubeis et al, 2014; Wang et al, 2016;

562   Yuen et al, 2016; Li et al, 2017; Guo et al, 2019; Leblond, et al, 2019). Here we provide the first

563   functional evidence demonstrating that Kirrel3 variants could cause disease.

564   Interestingly, not all of the missense variants studied present a phenotype. Our newly reported

565   M673I variant performs similar to wild-type Kirrel3 in all of the assays presented here. While this

566   negative result could mean this particular variant is not disease causing, it is also possible that the

567   variant requires a second mutation in another unidentified gene to impair its function or that our

568   current set of tests for Kirrel3 function have not yet revealed the cellular phenotypes caused by this

569   variant. For example, because CA1 neurons do not normally express Kirrel3, we would not expect this

570   assay to identify dominant negative mutations (discussed further below), only loss-of-function

571   mutations. Thus, M673I could function as a dominant negative and we are in the process of developing

572   new assays to test this class of mutations. Nonetheless, 5 of 6 tested disease-associated Kirrel3 variants

573   have impaired function in our assays, providing the first functional evidence that most disease-

574   associated Kirrel3 variants could cause neurodevelopmental disorders.

575   Most disease-associated Kirrel3 variants are rare, spontaneous mutations for which patients are

576   heterozygous. If these variants cause disease then Kirrel3 is likely haploinsufficient and/or disease-

577   associated variants act as dominant negative proteins. In support of haploinsufficiency, an interstitial

578   deletion on part of chromosome 11, which leads to a complete loss of one copy of Kirrel3 along with

579   other genes, is associated with Jacobsen syndrome, a developmental disorder with frequent

580   neurological symptoms including ASD, epilepsy, and intellectual disability (Guerin et al., 2012).

581   Furthermore, Kirrel3 has a pLI score, a probability measure that a gene is intolerant to heterozygous loss

582   of function variation, of 0.97 suggesting haploinsufficiency for loss of function variants (gnomAD

583   database https://gnomad.broadinstitute.org/; Lek et al, 2016). On the other hand, we find that all

584   missense variants tested localize to the cell surface at synapses similar to wild-type Kirrel3, suggesting

585   that Kirrel3 variants could interact in a dominant negative fashion by sequestering Kirrel3 binding

586   partners. Future work is needed to determine the precise mechanism of Kirrel3 and each variant in vivo,

587   but results from this study provide a critical foundation that Kirrel3 variants are likely bona fide disease

588   risk factors.

589   The study of Kirrel3 has strong potential to contribute to our broader understanding of the cellular

590   and circuit defects underlying ASD. Hundreds of genes are implicated as ASD risk factors but relatively

591   few have been the focus of intense study. Many commonly studied ASD risk genes are either

592   ubiquitously expressed throughout the body (TSC1, PTEN, MECP2, CHD8) or by many neurons across

593   most regions in the brain (DSCAM, NLGN3, SYNGAP1, SHANK3). This makes it difficult to identify the

594   essential cell and circuit level changes driving disorders such as ASD and ID, and any future therapeutics

595   based on widely expressed gene pathways are likely to have many adverse side effects. In contrast,

596   Kirrel3 is expressed by a relatively limited and specific subset of cell types (Lein et al., 2007; Allen

597   Institute for Brain Science, 2004; Allen institute for brain science, 2010; Hawrylycz et al., 2012; Martin et

598   al., 2015; Roh et al., 2017). Thus, understanding the mechanism of Kirrel3 in synapse formation and

599   function could point to a core set of synapse and circuit changes underlying some forms of ASD and ID.

600

601   **REFERENCES**

602   Abrahams BS, Arking DE, Campbell DB, Mefford HC, Morrow EM, Weiss LA, Menashe I, Wadkins T,

603   Banerjee-Basu S, Packer A (2013) SFARI Gene 2.0: a community-driven knowledgebase for the

604   autism spectrum disorders (ASDs). Molecular Autism 4:36.

605   Acsády L, Kamondi A, Sík A, Freund T, Buzsáki G (1998) GABAergic Cells Are the Major Postsynaptic

606   Targets of Mossy Fibers in the Rat Hippocampus. J Neurosci 18:3386–3403.

607   Allen Institute for Brain Science (2004). Allen Mouse Brain Atlas. Available at: https://mouse.brain-

608   map.org/ [Accessed December 17, 2019].

609   Allen Institute for Brain Science (2010). Allen Human Brain Atlas. Available at: https://human.brain-

610   map.org/ [Accessed December 17, 2019].

611   American Psychiatric Association (2013) Diagnostic and statistical manual of mental disorders: DSM-5.

612   Washington, DC: American Psychiatric Association.

613   Bai D et al. (2019) Association of Genetic and Environmental Factors With Autism in a 5-Country Cohort.

614   JAMA Psychiatry 76:1035–1043.

615   Banerjee-Basu S, Packer A (2010) SFARI Gene: an evolving database for the autism research community.

616   Disease Models & Mechanisms 3:133–135.

617   Basu R, Duan X, Taylor MR, Martin EA, Muralidhar S, Wang Y, Gangi-Wellman L, Das SC, Yamagata M,

618   West PJ, Sanes JR, Williams ME (2017) Heterophilic Type II Cadherins Are Required for High-

619   Magnitude Synaptic Potentiation in the Hippocampus. Neuron 96:160-176.e8.

620   Ben-David E, Shifman S (2012) Networks of neuronal genes affected by common and rare variants in

621   autism spectrum disorders. PLoS Genet 8:e1002556.

622   Benson DL, Colman DR, Huntley GW (2001) Molecules, maps and synapse specificity. Nat Rev Neurosci

623   2:899–909.

624   Bhalla K, Luo Y, Buchan T, Beachem MA, Guzauskas GF, Ladd S, Bratcher SJ, Schroer RJ, Balsamo J,

625   DuPont BR, Lilien J, Srivastava AK (2008) Alterations in CDH15 and Kirrel3 in Patients with Mild to

626   Severe Intellectual Disability. The American Journal of Human Genetics 83:703–713.

627   Biederer T, Scheiffele P (2007) Mixed-culture assays for analyzing neuronal synapse formation. Nat

628   Protoc 2:670–676.

629   Bischofberger J, Engel D, Frotscher M, Jonas P (2006) Timing and efficacy of transmitter release at mossy

630   fiber synapses in the hippocampal network. Pflugers Arch - Eur J Physiol 453:361–372.

631   Brignall AC, Raja R, Phen A, Prince JEA, Dumontier E, Cloutier J-F (2018) Loss of Kirrel family members

632   alters glomerular structure and synapse numbers in the accessory olfactory bulb. Brain Struct Funct

633   223:307–319.

634   Bulchand S, Menon SD, George SE, Chia W (2010) The Intracellular Domain of Dumbfounded Affects

635   Myoblast Fusion Efficiency and Interacts with Rolling Pebbles and Loner. PLOS ONE 5:e9374.

636   Chao DL, Shen K (2008) Functional dissection of SYG-1 and SYG-2, cell adhesion molecules required for

637   selective synaptogenesis in C. elegans. Molecular and Cellular Neuroscience 39:248–257.

638   Chia PH, Chen B, Li P, Rosen MK, Shen K (2014) Local F-actin Network Links Synapse Formation and Axon

639   Branching. Cell 156:208–220.

640   Chicurel ME, Harris KM (1992) Three-dimensional analysis of the structure and composition of CA3

641   branched dendritic spines and their synaptic relationships with mossy fiber boutons in the rat

642   hippocampus. Journal of Comparative Neurology 325:169–182.

643   Chih B, Afridi SK, Clark L, Scheiffele P (2004) Disorder-associated mutations lead to functional

644   inactivation of neuroligins. Hum Mol Genet 13:1471–1477.

645   Choi SY, Han K, Cutforth T, Chung W, Park H, Lee D, Kim R, Kim M-H, Choi Y, Shen K, Kim E (2015) Mice

646   lacking the synaptic adhesion molecule Neph2/Kirrel3 display moderate hyperactivity and

647   defective novel object preference. Front Cell Neurosci 9 Available at:

648   https://www.frontiersin.org/articles/10.3389/fncel.2015.00283/full [Accessed December 5, 2019].

649   Constantino JN, Charman T (2016) Diagnosis of autism spectrum disorder: reconciling the syndrome, its

650   diverse origins, and variation in expression. The Lancet Neurology 15:279–291.

651   Ding M, Chao D, Wang G, Shen K (2007) Spatial Regulation of an E3 Ubiquitin Ligase Directs Selective

652   Synapse Elimination. Science 317:947–951.

653   Ferland RJ, Cherry TJ, Preware PO, Morrisey EE, Walsh CA (2003) Characterization of Foxp2 and Foxp1

654   mRNA and protein in the developing and mature brain. Journal of Comparative Neurology

655   460:266–279.

656   Gerke P, Sellin L, Kretz O, Petraschka D, Zentgraf H, Benzing T, Walz G (2005) NEPH2 Is Located at the

657   Glomerular Slit Diaphragm, Interacts with Nephrin and Is Cleaved from Podocytes by

658   Metalloproteinases. JASN 16:1693–1702.

659   Gerke P, Benzing T, Höhne M, Kispert A, Frotscher M, Walz G, Kretz O (2006) Neuronal expression and

660   interaction with the synaptic protein CASK suggest a role for Neph1 and Neph2 in synaptogenesis.

661   Journal of Comparative Neurology 498:466–475.

662   Geschwind DH, State MW (2015) Gene hunting in autism spectrum disorder: on the path to precision

663   medicine. The Lancet Neurology 14:1109-1120

664   Graf ER, Zhang X, Jin S-X, Linhoff MW, Craig AM (2004) Neurexins Induce Differentiation of GABA and

665   Glutamate Postsynaptic Specializations via Neuroligins. Cell 119:1013–1026.

666   Guerin A, Stavropoulos DJ, Diab Y, Chénier S, Christensen H, Kahr WH, Babul-Hirji R, Chitayat D (2012)

667   Interstitial deletion of 11q-implicating the Kirrel3 gene in the neurocognitive delay associated with

668   Jacobsen syndrome. American Journal of Medical Genetics Part A 158A:2551–2556.

669   Guo H, Duyzend MH, Coe BP, Baker C, Hoekzema K, Gerdts J, Turner TN, Zody MC, Beighley JS, Murali SC,

670   Nelson BJ, University of Washington Center for Mendelian Genomics, Bamshad MJ, Nickerson DA,

671   Bernier RA, Eichler EE (2019) Genome sequencing identifies multiple deleterious variants in autism

672   patients with more severe phenotypes. Genet Med 21:1611–1620.

673   Hawrylycz MJ et al. (2012) An anatomically comprehensive atlas of the adult human brain

674   transcriptome. Nature 489:391–399.

675   Hisaoka T, Komori T, Kitamura T, Morikawa Y (2018) Abnormal behaviours relevant to

676   neurodevelopmental disorders in Kirrel3-knockout mice. Sci Rep 8:1–12.

677   Huber TB, Schmidts M, Gerke P, Schermer B, Zahn A, Hartleben B, Sellin L, Walz G, Benzing T (2003) The

678   Carboxyl Terminus of Neph Family Members Binds to the PDZ Domain Protein Zonula Occludens-1.

679   J Biol Chem 278:13417–13421.

680   Iossifov I et al. (2014) The contribution of de novo coding mutations to autism spectrum disorder.

681   Nature 515:216–221.

682   Jaco AD, Lin MZ, Dubi N, Comoletti D, Miller MT, Camp S, Ellisman M, Butko MT, Tsien RY, Taylor P

683   (2010) Neuroligin Trafficking Deficiencies Arising from Mutations in the α/β-Hydrolase Fold Protein

684   Family. J Biol Chem 285:28674–28682.

685   Kaminsky EB et al. (2011) An evidence-based approach to establish the functional and clinical

686   significance of copy number variants in intellectual and developmental disabilities. Genetics in

687   Medicine 13:777–784.

688   Komori T, Gyobu H, Ueno H, Kitamura T, Senba E, Morikawa Y (2008) Expression of kin of irregular

689   chiasm-like 3/mKirre in proprioceptive neurons of the dorsal root ganglia and its interaction with

690   nephrin in muscle spindles. Journal of Comparative Neurology 511:92–108.

691   Kreisköther N, Reichert N, Buttgereit D, Hertenstein A, Fischbach K-F, Renkawitz-Pohl R (2006)

692   Drosophila Rolling pebbles colocalises and putatively interacts with alpha-Actinin and the Sls

693   isoform Zormin in the Z-discs of the sarcomere and with Dumbfounded/Kirre, alpha-Actinin and

694   Zormin in the terminal Z-discs. J Muscle Res Cell Motil 27:93.

695   Leblond CS, Cliquet F, Carton C, Huguet G, Mathieu A, Kergrohen T, Buratti J, Lemière N, Cuisset L,

696   Bienvenu T, Boland A, Deleuze J-F, Stora T, Biskupstoe R, Halling J, Andorsdóttir G, Billstedt E,

697   Gillberg C, Bourgeron T (2019) Both rare and common genetic variants contribute to autism in the

698   Faroe Islands. NPJ Genom Med 4 Available at:

699   https://www.ncbi.nlm.nih.gov/pmc/articles/PMC6341098/ [Accessed December 15, 2019].

700 Lein ES et al. (2007) Genome-wide atlas of gene expression in the adult mouse brain. Nature 445:168–

701   176.

702 Lek M et al. (2016) Analysis of protein-coding genetic variation in 60,706 humans. Nature 536:285–291.

703 Li J, Wang L, Guo H, Shi L, Zhang K, Tang M, Hu S, Dong S, Liu Y, Wang T, Yu P, He X, Hu Z, Zhao J, Liu C,

704   Sun ZS, Xia K (2017) Targeted sequencing and functional analysis reveal brain-size-related genes

705   and their networks in autism spectrum disorders. Mol Psychiatry 22:1282–1290.

706 Madeira F, Park Y mi, Lee J, Buso N, Gur T, Madhusoodanan N, Basutkar P, Tivey ARN, Potter SC, Finn RD,

707   Lopez R (2019) The EMBL-EBI search and sequence analysis tools APIs in 2019. Nucleic Acids Res

708   47:W636–W641.

709 Martin EA, Muralidhar S, Wang Z, Cervantes DC, Basu R, Taylor MR, Hunter J, Cutforth T, Wilke SA,

710   Ghosh A, Williams ME (2015) The intellectual disability gene Kirrel3 regulates target-specific mossy

711   fiber synapse development in the hippocampus Davis GW, ed. eLife 4:e09395.

712 Martin EA, Woodruff D, Rawson RL, Williams ME (2017) Examining Hippocampal Mossy Fiber Synapses

713   by 3D Electron Microscopy in Wild-type and Kirrel3 Knockout Mice. eNeuro 4 Available at:

714   https://www.eneuro.org/content/4/3/ENEURO.0088-17.2017 [Accessed December 4, 2019].

715 Michaelson JJ et al. (2012) Whole-Genome Sequencing in Autism Identifies Hot Spots for De Novo

716   Germline Mutation. Cell 151:1431–1442.

717 Neale BM et al. (2012) Patterns and rates of exonic de novo mutations in autism spectrum disorders.

718   Nature 485:242–245.

719 Özkan E, Chia PH, Wang RR, Goriatcheva N, Borek D, Otwinowski Z, Walz T, Shen K, Garcia KC (2014)

720   Extracellular Architecture of the SYG-1/SYG-2 Adhesion Complex Instructs Synaptogenesis. Cell

721   156:482–494.

722   Prince JEA, Brignall AC, Cutforth T, Shen K, Cloutier J-F (2013) Kirrel3 is required for the coalescence of

723   vomeronasal sensory neuron axons into glomeruli and for male-male aggression. Development

724   140:2398–2408.

725   Richards S, Aziz N, Bale S, Bick D, Das S, Gastier-Foster J, Grody WW, Hegde M, Lyon E, Spector E,

726   Voelkerding K, Rehm HL (2015) Standards and guidelines for the interpretation of sequence

727   variants: a joint consensus recommendation of the American College of Medical Genetics and

728   Genomics and the Association for Molecular Pathology. Genet Med 17:405–423.

729   Roh JD et al. (2017) Increased Excitatory Synaptic Transmission of Dentate Granule Neurons in Mice

730   Lacking PSD-95-Interacting Adhesion Molecule Neph2/Kirrel3 during the Early Postnatal Period.

731   Front Mol Neurosci 10 Available at:

732   https://www.frontiersin.org/articles/10.3389/fnmol.2017.00081/full [Accessed December 6,

733   2019].

734   Rubeis SD et al. (2014) Synaptic, transcriptional and chromatin genes disrupted in autism. Nature

735   515:209–215.

736   Sandin S, Lichtenstein P, Kuja-Halkola R, Hultman C, Larsson H, Reichenberg A (2017) The Heritability of

737   Autism Spectrum Disorder. JAMA 318:1182–1184.

738   Sanes JR, Yamagata M (2009) Many Paths to Synaptic Specificity. Annual Review of Cell and

739   Developmental Biology 25:161–195.

740   Scheiffele P, Fan J, Choih J, Fetter R, Serafini T (2000) Neuroligin Expressed in Nonneuronal Cells Triggers

741   Presynaptic Development in Contacting Axons. Cell 101:657–669.

742   Sellin L, Huber TB, Gerke P, Quack I, Pavenstädt H, Walz G (2002) NEPH1 defines a novel family of

743   podocin interacting proteins. The FASEB Journal 17:115–117.

744   Serizawa S, Miyamichi K, Takeuchi H, Yamagishi Y, Suzuki M, Sakano H (2006) A Neuronal Identity Code

745   for the Odorant Receptor-Specific and Activity-Dependent Axon Sorting. Cell 127:1057–1069.

746 Shen K, Bargmann CI (2003) The Immunoglobulin Superfamily Protein SYG-1 Determines the Location of

747   Specific Synapses in C. elegans. Cell 112:619–630.

748 Shen K, Fetter RD, Bargmann CI (2004) Synaptic Specificity Is Generated by the Synaptic Guidepost

749   Protein SYG-2 and Its Receptor, SYG-1. Cell 116:869–881.

750 Sperry RW (1963) Chemoaffinity in the orderly growth of nerve fiber patterns and connections. Proc Natl

751   Acad Sci U S A 50:703–710.

752 Südhof TC (2018) Towards an Understanding of Synapse Formation. Neuron 100:276–293.

753 Talkowski ME et al. (2012) Sequencing Chromosomal Abnormalities Reveals Neurodevelopmental Loci

754   that Confer Risk across Diagnostic Boundaries. Cell 149:525–537.

755 Tick B, Bolton P, Happé F, Rutter M, Rijsdijk F (2016) Heritability of autism spectrum disorders: a meta-

756   analysis of twin studies. Journal of Child Psychology and Psychiatry 57:585–595.

757 Vishnu S, Hertenstein A, Betschinger J, Knoblich JA, Gert de Couet H, Fischbach K-F (2006) The adaptor

758   protein X11Lα/Dmint1 interacts with the PDZ-binding domain of the cell recognition protein Rst in

759   Drosophila. Developmental Biology 289:296–307.

760 Völker LA, Maar BA, Guevara BAP, Bilkei-Gorzo A, Zimmer A, Brönneke H, Dafinger C, Bertsch S,

761   Wagener J-R, Schweizer H, Schermer B, Benzing T, Hoehne M (2018) Neph2/Kirrel3 regulates

762   sensory input, motor coordination, and home-cage activity in rodents. Genes, Brain and Behavior

763   17:e12516.

764 Wang T et al. (2016) De novo genic mutations among a Chinese autism spectrum disorder cohort. Nat

765   Commun 7:1–10.

766 Williams ME, Wilke SA, Daggett A, Davis E, Otto S, Ravi D, Ripley B, Bushong EA, Ellisman MH, Klein G,

767   Ghosh A (2011) Cadherin-9 Regulates Synapse-Specific Differentiation in the Developing

768   Hippocampus. Neuron 71:640–655.

769   Yuen RK et al. (2016) Genome-wide characteristics of de novo mutations in autism. NPJ Genom Med

770   1:16027.

771   Zhang C, Milunsky JM, Newton S, Ko J, Zhao G, Maher TA, Tager-Flusberg H, Bolliger MF, Carter AS,

772   Boucard AA, Powell CM, Südhof TC (2009) A Neuroligin-4 Missense Mutation Associated with

773   Autism Impairs Neuroligin-4 Folding and Endoplasmic Reticulum Export. J Neurosci 29:10843–

774   10854.

775

776   **FIGURE LEGENDS**

777   **Figure 1**. Ectopic Kirrel3 expression induces ectopic DG pre-synapses in cultured neurons. **A**, Schematic

778   of Kirrel3 (K3) protein. Ig; Immunoglobulin domain. **B**, Schematic of the gain-of-function assay design.

779   Top: In the control condition, a Kirrel3 positive DG neuron contacts a Kirrel3 negative CA1 dendrite and

780   does not form a pre-synapse. Bottom: A Kirrel3 positive DG neuron contacts a Kirrel3-transfected CA1

781   neuron allowing for a DG pre-synapse to form. **C**, Tiled 20x image of an adult mouse hippocampal

782   section immunostained with the CA1 marker Foxp1 (blue) and the presynaptic markers VGluT1 (green)

783   and SPO (red). Grayscale images below. In each image the white arrow indicates approximate CA3

784   border. Scale bars = 200μm. **D**, Dendrites from cultured rat CA1 dendrites transfected with GFP (left) or

785   GFP + Kirrel3 (right). GFP is not shown but is outlined in white. DG pre-synapses (yellow) are identified

786   by co-labelling of SPO (red) and VGluT1 (green). Arrows point to DG pre-synapses. Scale bar = 5 μm. **E**,

787   Quantification of DG pre-synapse density per length of CA1 dendrite and normalized to the GFP

788   condition. n=38-48 neurons (indicated in each bar) from 3 cultures, p=0.0027 (Mann Whitney test). **F**,

789   Quantification of CA synapse density per length of CA1 dendrite and normalized to the GFP condition.

790   n=38-48 neurons (indicated in each bar) from 3 cultures, p=0.9552 (Mann Whitney test). **G**,

791   Quantification of DG pre-synapse density per length of CA1 dendrite from Kirrel3 wild-type (WT) and

792   knockout (KO) cultures. All are normalized to the wild-type GFP condition. n=17-42 neurons (indicated in

793   each bar) from 3 cultures, WT: GFP vs GFP+Kirrel3 p=0.0088; KO: GFP vs GFP+Kirrel3, p=0.9560 (Two-

794   way ANOVA with Sidak's multiple comparisons, p= 0.0266; interaction) **H**, Schematic of WT versus KO

795   assay results suggesting that Kirrel3 must be present in both the pre- and postsynaptic neuron to induce

796   DG synapse formation. For F, and G, ns = not significant.

797

798   **Figure 2.** Kirrel3 expression does not increase axon-dendrite contact in cultured neurons. **A,**

799   Representative images of neurons transfected with GFP and Kirrel3 (green) contacted by mCherry (mCh)

800   labeled axons with (top) or without (bottom) Kirrel3. Scale bar = 10µm. **B**, Quantification of axon contact

801   assay normalized to the Kirrel3-negative mCherry-labelled axon condition. Axon contact index is the

802   area of mCherry positive axon per area GFP positive cell. n=22-29 neurons (indicated in each bar) from 2

803   cultures, p=0.2445 (Mann Whitney Test). ns = not significant.

804

805   **Figure 3**. Kirrel3 in a non-neuronal cell is not sufficient to mediate synapse formation. **A**, Representative

806   images of the presynaptic neuron/HEK293 co-culture assay. Cultures were immunostained for GFP

807   (blue) to label transfected HEK293 cells and VGluT1 (red) to label pre-synapses. Transfection conditions

808   are indicated on each image. Nlgn1 = Neuroligin-1, K3 = Kirrel3. Arrow in bottom right panel points to an

809   outline of a FLAG-Kirrel3 positive axon **B**, Quantification of presynaptic hemisynapse density from the

810   co-culture assay normalized to the GFP-only negative control (GFP). n=32-61 cells (indicated in each bar)

811   from 2 cultures, GFP vs Nlgn1 p=0.0074; GFP vs Kirrel3, p=0.3988; GFP vs K3+K3 p>0.9999 (One-way

812   ANOVA Kruskal-Wallis test, p=0.0226, with Dunn's multiple comparisons). **C,** Images of the postsynaptic

813   hemisynapse density from the co-culture assay. Cultures were immunostained with GFP (blue), vGluT1

814   (red) and PSD-95 (green). Postsynaptic hemisynapses are labelled by PSD-95 alone with no VGluT1.

815   Nrxn1 = Neurexin-1. **D**, Quantification of postsynaptic hemisynapse density from co-culture assay

816   normalized to the GFP-only negative control. n=19-20 cells (indicated in each bar) from one culture, GFP

817   vs Nrxn1 p=0.0252; GFP vs Kirrel3 p>0.9999 (One-way ANOVA Kruskal-Wallis test, p=0.0256, with Dunn's

818   multiple comparisons). Scale bar in A and C = 20μm.

819

820   **Figure 4**. Kirrel3 missense variants show normal surface localization. **A**, Schematic of Kirrel3 protein with

821   approximate positions of disease-associated missense variants. Variants tested in this study are

822   magenta. **B**, Representative images of CHO cells transfected with mCh-2A-FLAG-Kirrel3 variants. Cells

823   were live-labelled with chicken-anti-FLAG (magenta) to show extracellular (EC) Kirrel3 protein and then

824   permeabilized and stained with mouse-anti-FLAG (orange) to show intracellular (IC) Kirrel3 protein. Cell

825   area was determined by GFP expression and is depicted by a white outline. Scale bar = 15μm. **C**,

826   Quantification of EC/IC Kirrel3 protein levels normalized to wild-type Kirrel3. n=9 cells each from 3

827   cultures, p=0.4424 (One-way ANOVA). **D**, Representative images showing a dendrite from a mCherry-2A-

828   FLAG-Kirrel3 wild-type transfected neuron. EC FLAG-Kirrel3 (yellow) localizes adjacent to juxtaposed

829   synaptic markers VGluT1 (blue) and PSD-95 (red). mCherry-2A (magenta) serves as a cell marker. Scale

830   bar = 4μm. **E**, Quantification of the percent of synapses (juxtaposed VGluT1$^+$, PSD-95$^+$ puncta) with

831   adjacent FLAG-Kirrel3 proteins for each variant. n=9-19 neurons (indicated in each bar) from two

832   cultures, p=0.3197 (One-way ANOVA Kruskal-Wallis test). ns = not significant

833

834   **Figure 5**. Missense variants attenuate Kirrel3-mediated synapse formation. **A**, Representative images of

835   CA1 dendrites transfected with GFP only (GFP), or GFP and indicated FLAG-Kirrel3 variants. Outlines

836   show dendrite area as determined from GFP expression. DG pre-synapses (yellow) are identified by co-

837   labelling of SPO (red) and VGluT1 (green). Arrows point to DG pre-synapses. Scale bar = 5μm. **B**,

838   Quantification of DG pre-synapse density on CA1 dendrites normalized to wild-type Kirrel3 and with

839   multiple comparisons to wild-type Kirrel3. n=30-55 neurons (indicated in each bar) from 3-5 cultures,

840   (One-way ANOVA Kruskal-Wallis test with multiple comparisons to WT Kirrel3). **C**, Same data as

841   presented in B but shown normalized to GFP and with multiple comparisons to GFP. See results section

842   for specific p-values but *p<0.05, **p<0.01, and ****p<0.0001.

843

844   **Figure 6**. Kirrel3 missense variants fail to induce synapse development via different mechanisms. **A**,

845   Immunoblot of untransfected CHO and HEK293 cell lysates showing no detectable endogenous Kirrel3

846   expression. CHO cells transfected with FLAG-Kirrel3-pBOS were used as a positive control. **B**,

847   Representative images from CHO aggregation assay showing CHO cells transfected with mCherry alone

848   as a negative control (Ctrl), mCherry-2A-Kirrel3-wild-type (WT K3), or mCherry-2A-Kirrel3 variants.

849   mCherry (mCh) signal is shown in red, DAPI in blue. Scale bar = 50µm. **C**, Quantification of CHO cell

850   aggregation assay normalized to wild-type Kirrel3. n=8-18 wells (indicated in each bar) from 3 cultures.

851   See results section for specific p-values. *p<0.05, ***p<0.001, ****p<0.0001. **D**, K-means clustering of

852   wild-type Kirrel3, missense variants, and negative control based on their ability to aggregate CHO cells

853   and induce DG pre-synapse formation using mean rank values normalized to wild-type Kirrel3 for each

854   condition from the two assays presented in figures 5B and 6C.

855
856   **Table 1**: Kirrel3 missense variants associated with neurodevelopmental disorders.

Variant ID	Amino Acid Change	Associated Conditions	Reference
rs182260035	Val30Met	ASD	Rubeis et al, 2014
rs119462978	Arg40Trp	ID	Bhalla et al, 2008
rs779979146	Arg161His	ASD	Iossifov et al, 2014; Yuen et al, 2016
rs376743687	His171Gln	ASD	Rubeis et al, 2014
rs572991045	Arg205Gln	ASD	Rubeis et al, 2014
	Lys212Asn	ASD	Rubeis et al, 2014
rs372786849	Ser241Leu	ASD	Li et al, 2017
rs201725914	Val303Ala	ASD	Rubeis et al, 2014
rs114378922	Arg336Gln	ID	Bhalla et al, 2008
	Trp358Cys	ASD	Li et al, 2017
rs201882059	Ala393Thr	ASD	Wang et al, 2016
rs369363937	Ala393Val	ASD	Wang et al, 2016
rs1053637755	Gln428Lys	ASD	Li et al, 2017
rs760499655	Pro446Leu	ASD	Li et al, 2017

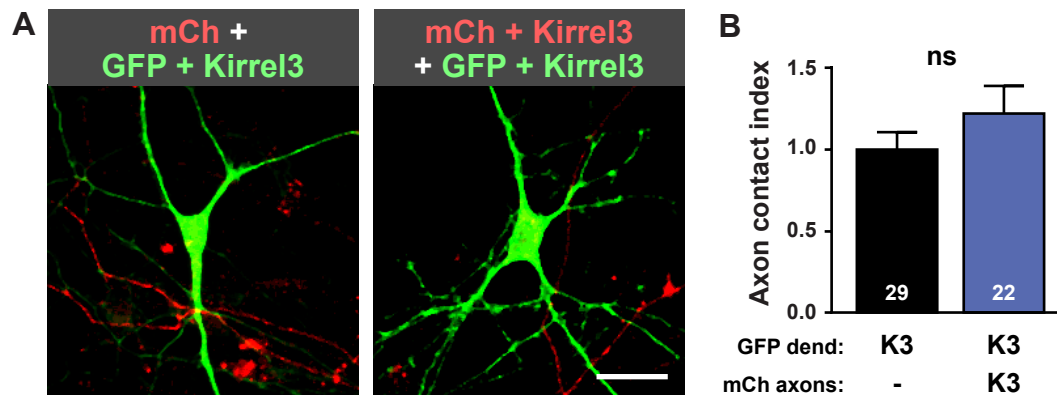|	Arg562Leu	ASD	Leblond, et al, 2019
rs773312950	Arg650His	ASD	Guo et al, 2019
rs1057519593	M6731I	ID, ADHD	This study
rs119462980	Val731Phe	ID	Bhalla et al, 2008

857

858

Fig 1. Ectopic Kirrel3 expression induces ectopic pre-synapses in cultured neurons
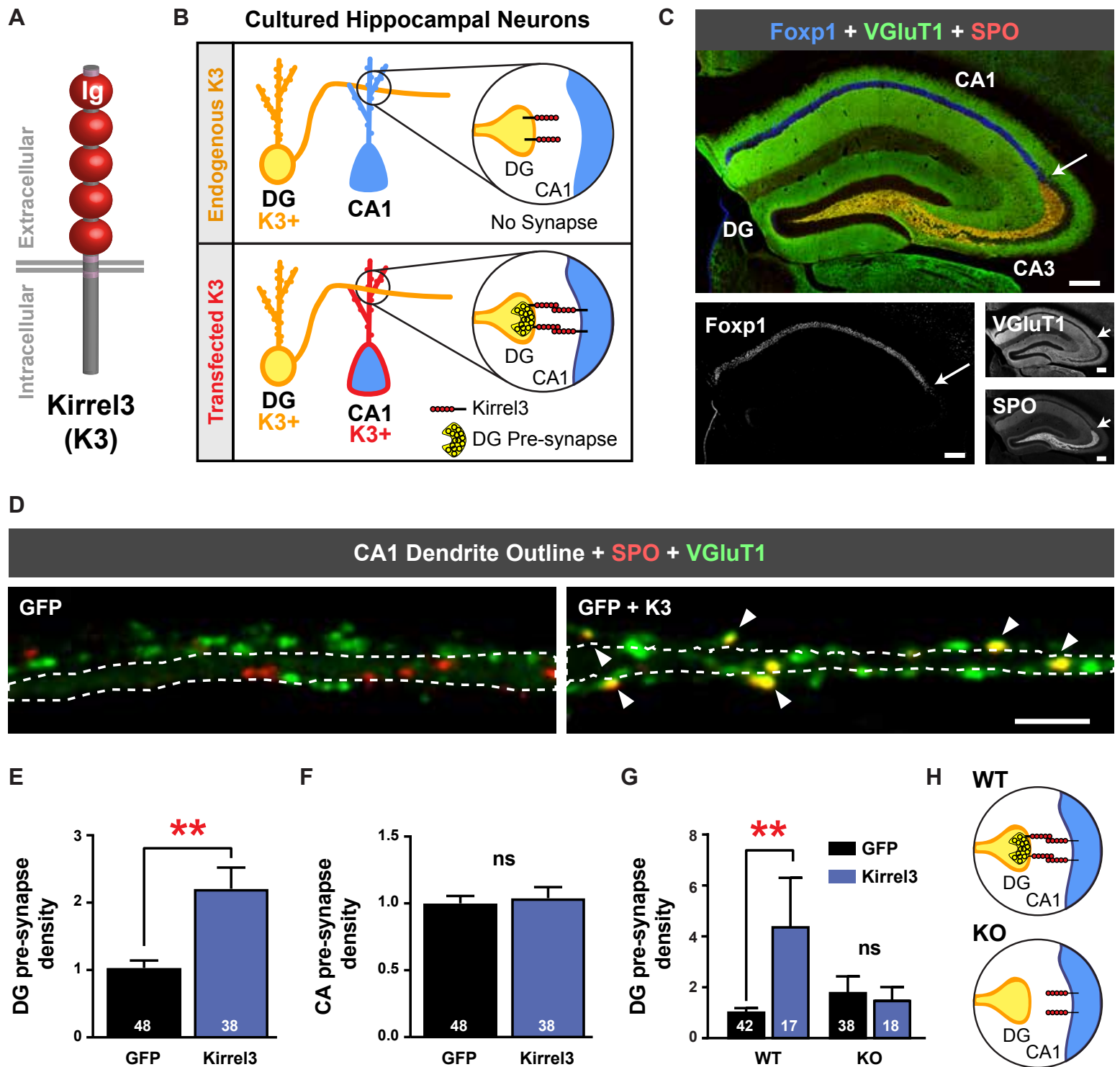
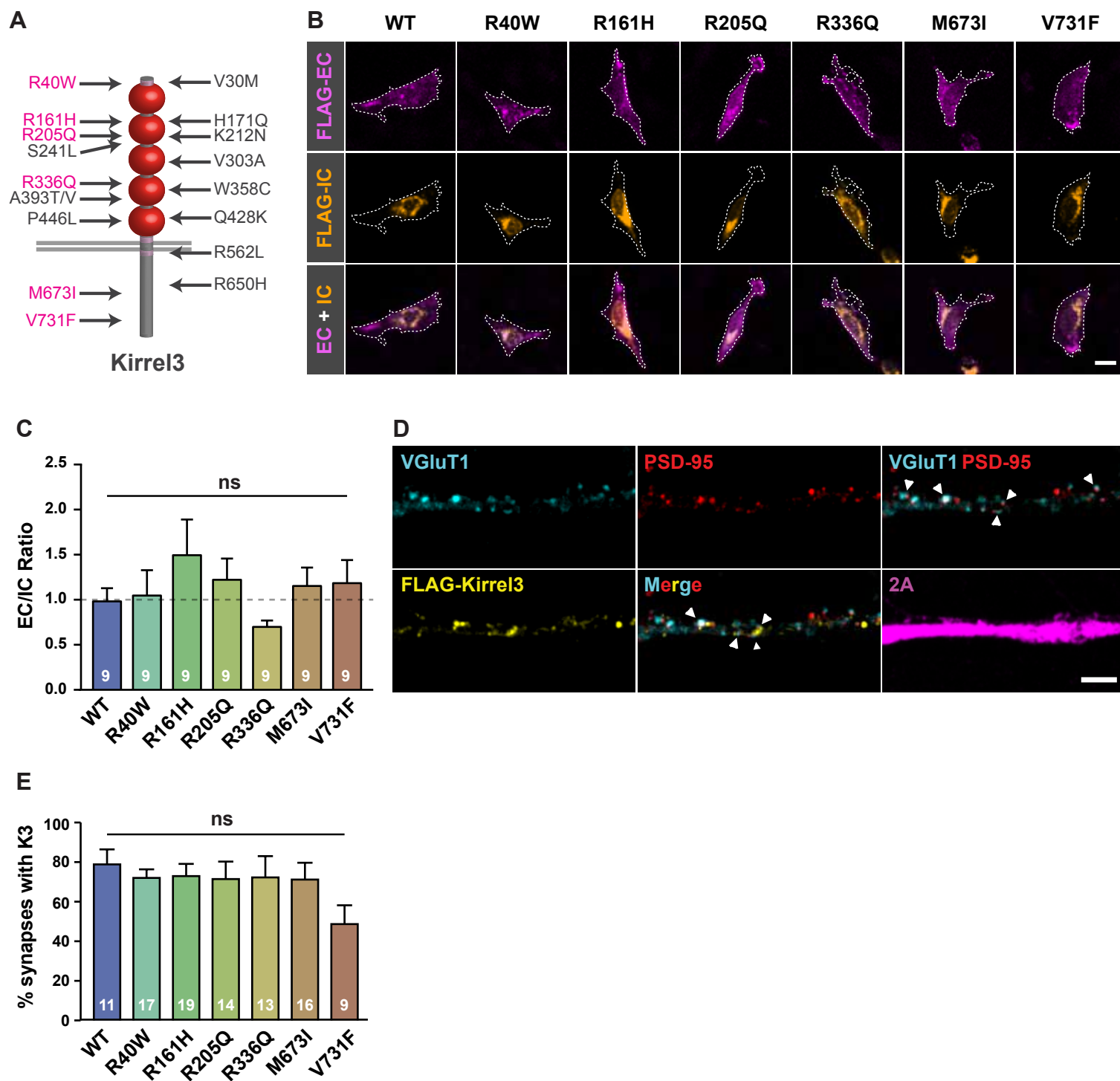**Fig 2. Kirrel3 expression does not increase axon-dendritic contact in cultured neurons**

Fig 3. Kirrel3 in a non-neuronal cell is not sufficient to mediate synapse development
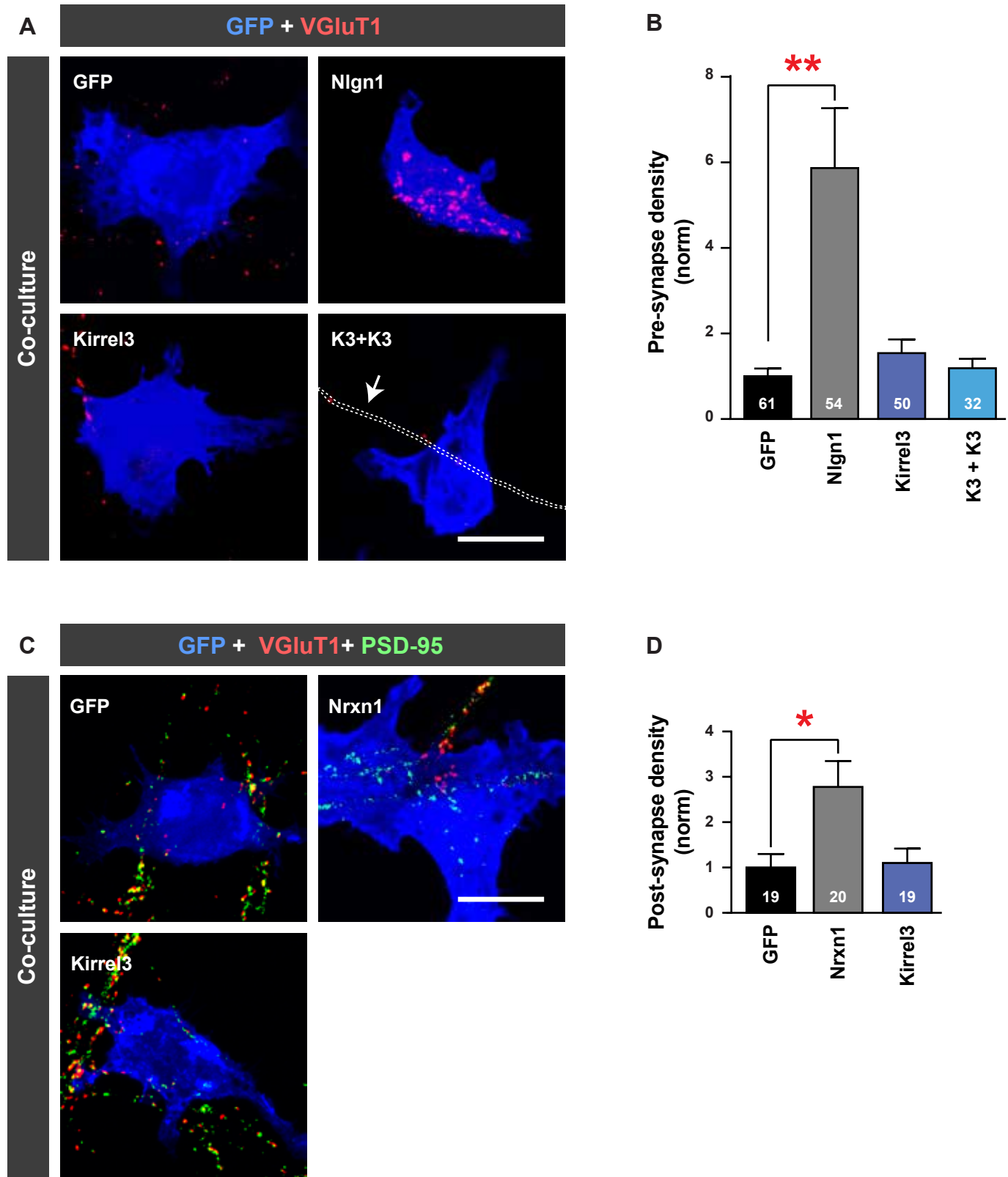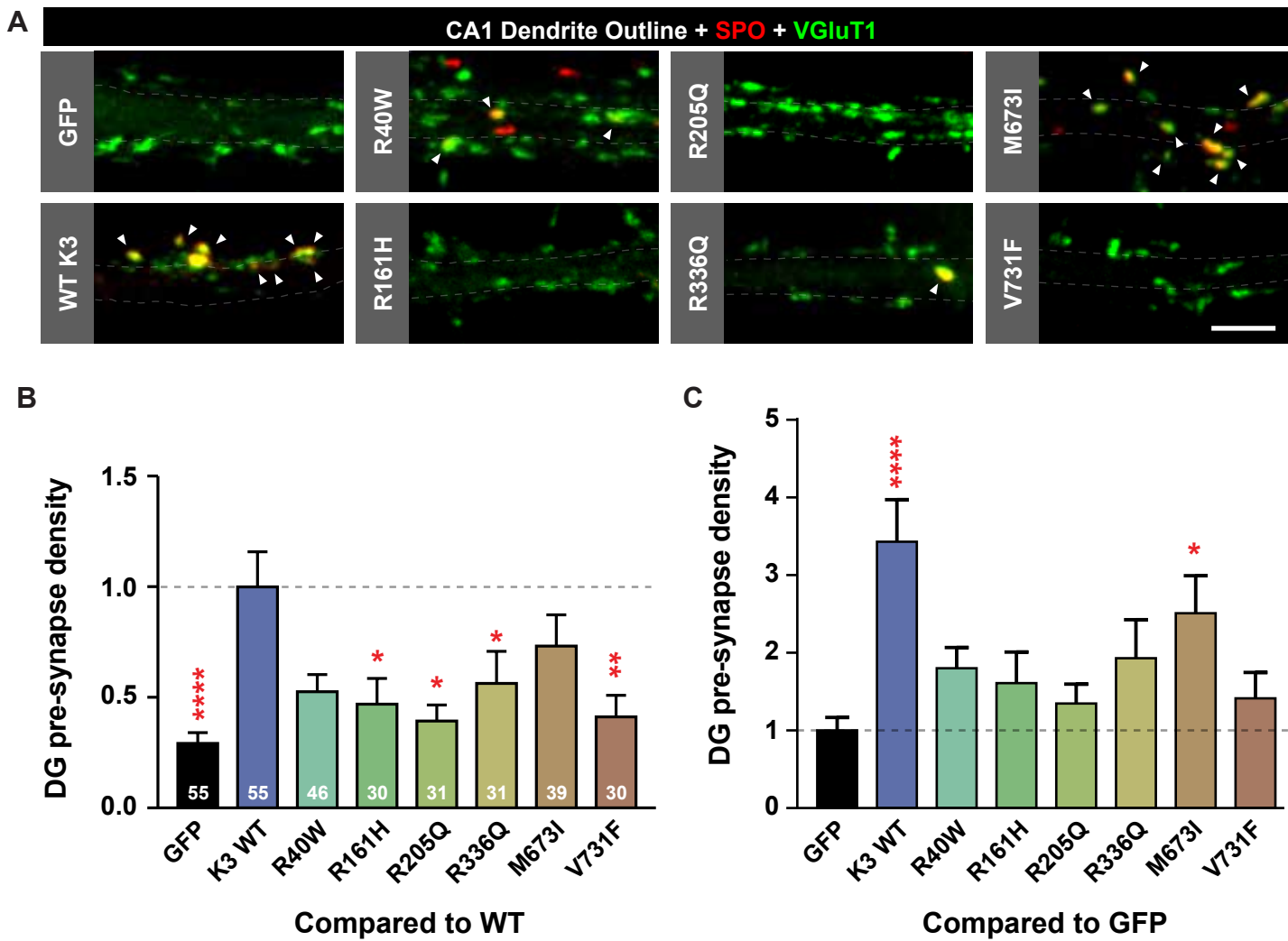
Fig 4: Kirrel3 missense variants show normal surface localization

Fig 5: Missense variants attenuate Kirrel3-mediated synapse formation

Fig 6. Kirrel3 missense variants fail to induce synapse development via different mechanisms